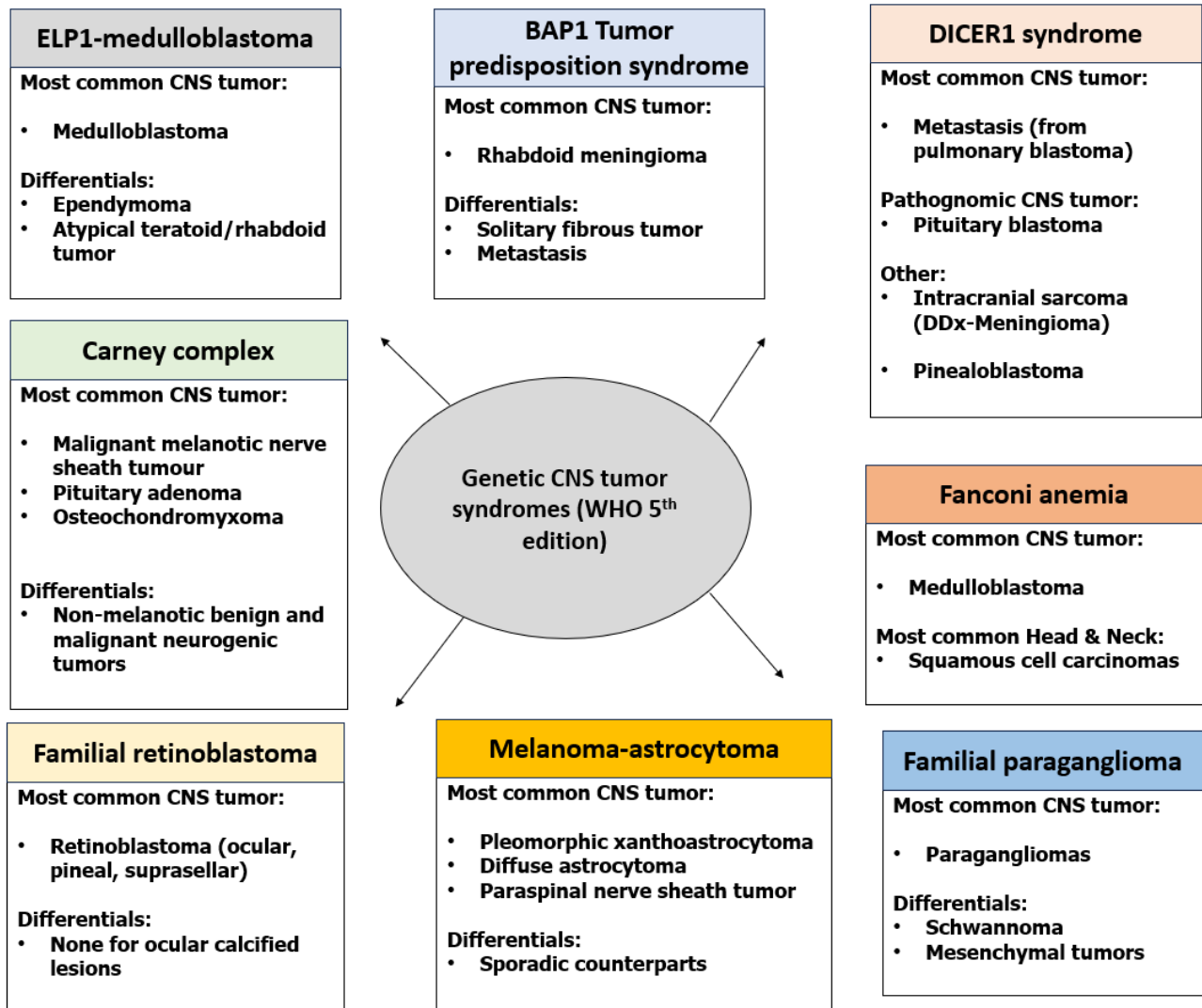


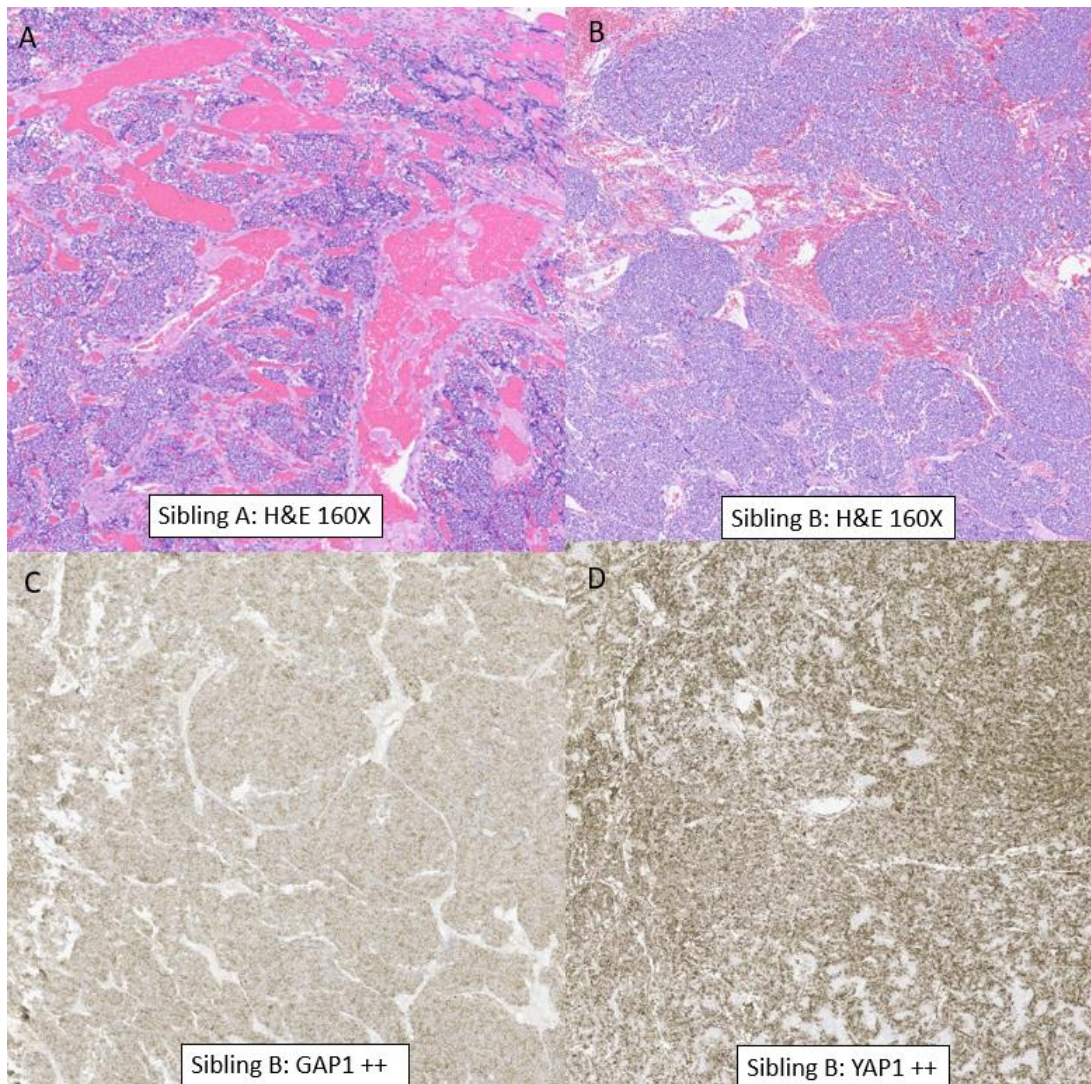
Supplemental

Fig 1s



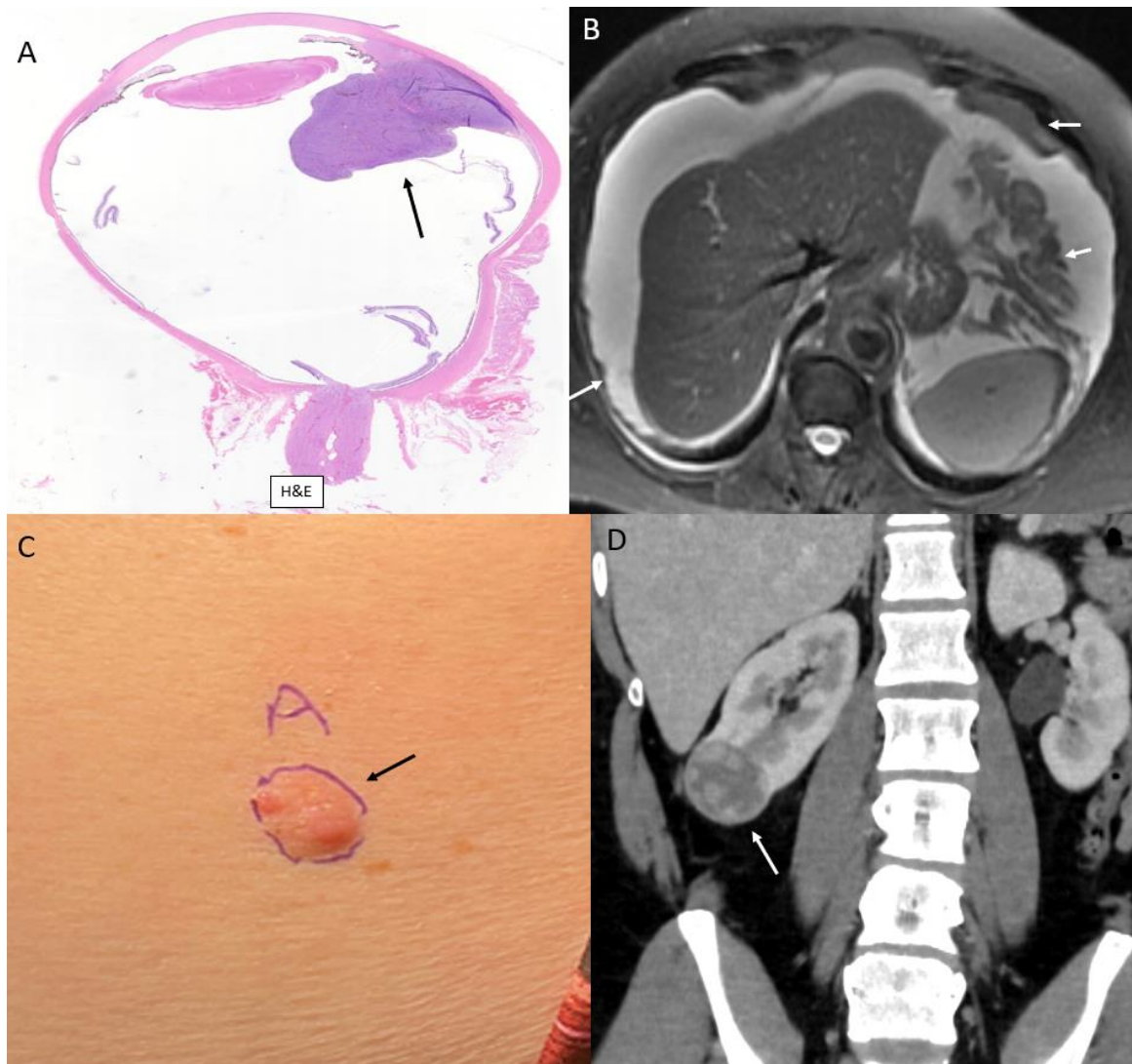
Diagrammatic representation of the most common CNS tumors in the eight Who 5th edition genetic tumor syndromes and their radiographic differentials.

Fig 2s



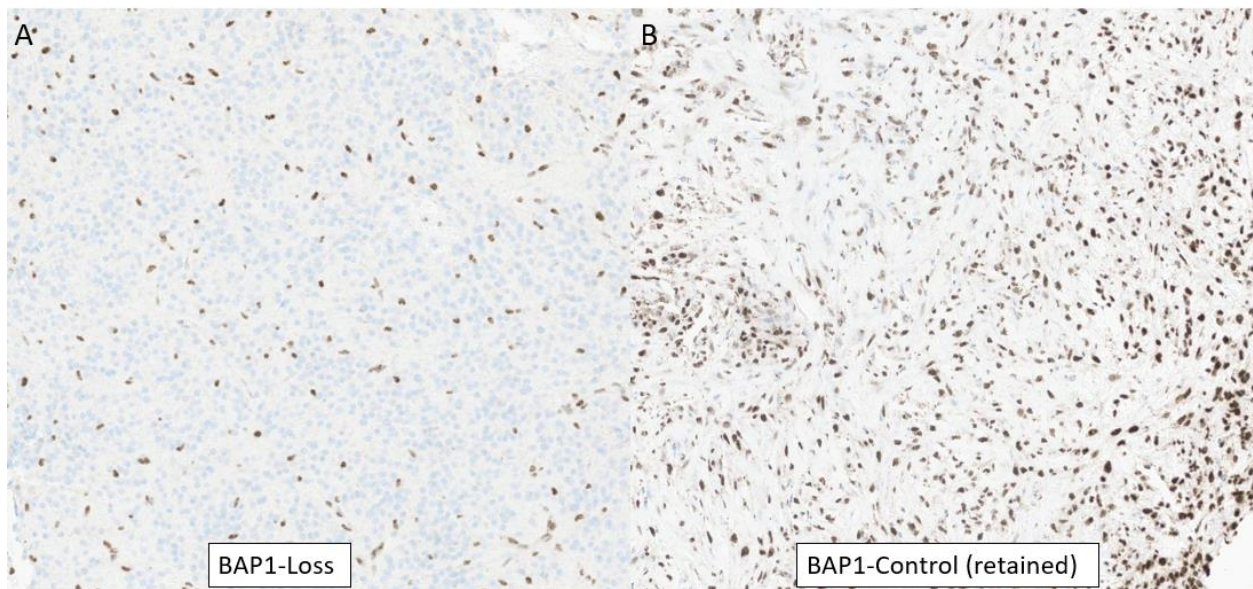
ELP1-related medulloblastomas in siblings. A 6-year-old boy (sibling A) with large cell/anaplastic pattern WHO grade 4, SHH activated (TP53 wild type) medulloblastoma (A). Patient's older brother, 18-year-old boy (sibling B), was diagnosed with similar tumor, seven years later. Pathology revealed SHH activated (TP53 wild type) medulloblastoma with desmoplastic/nodular morphology (B). Immunohistochemical studies (C,D) reveal nuclear and cytoplasmic expression of YAP and cytoplasmic expression of GAB1. Immunoreactivity for GAB1 characterizes only SHH tumors. These findings are consistent with SHH molecular subgroup medulloblastoma. Neurooncology genetic panel (next-generation sequencing) in both siblings showed biallelic inactivation of ELP1 due to somatic loss of chromosome arm 9q along with homozygous deletion of tumor suppressor gene PTCH1, confirming ELP1 germline mutation. Both siblings remain disease free (9 years post-surgery for sibling A, and 1 year for sibling B).

Fig 3s



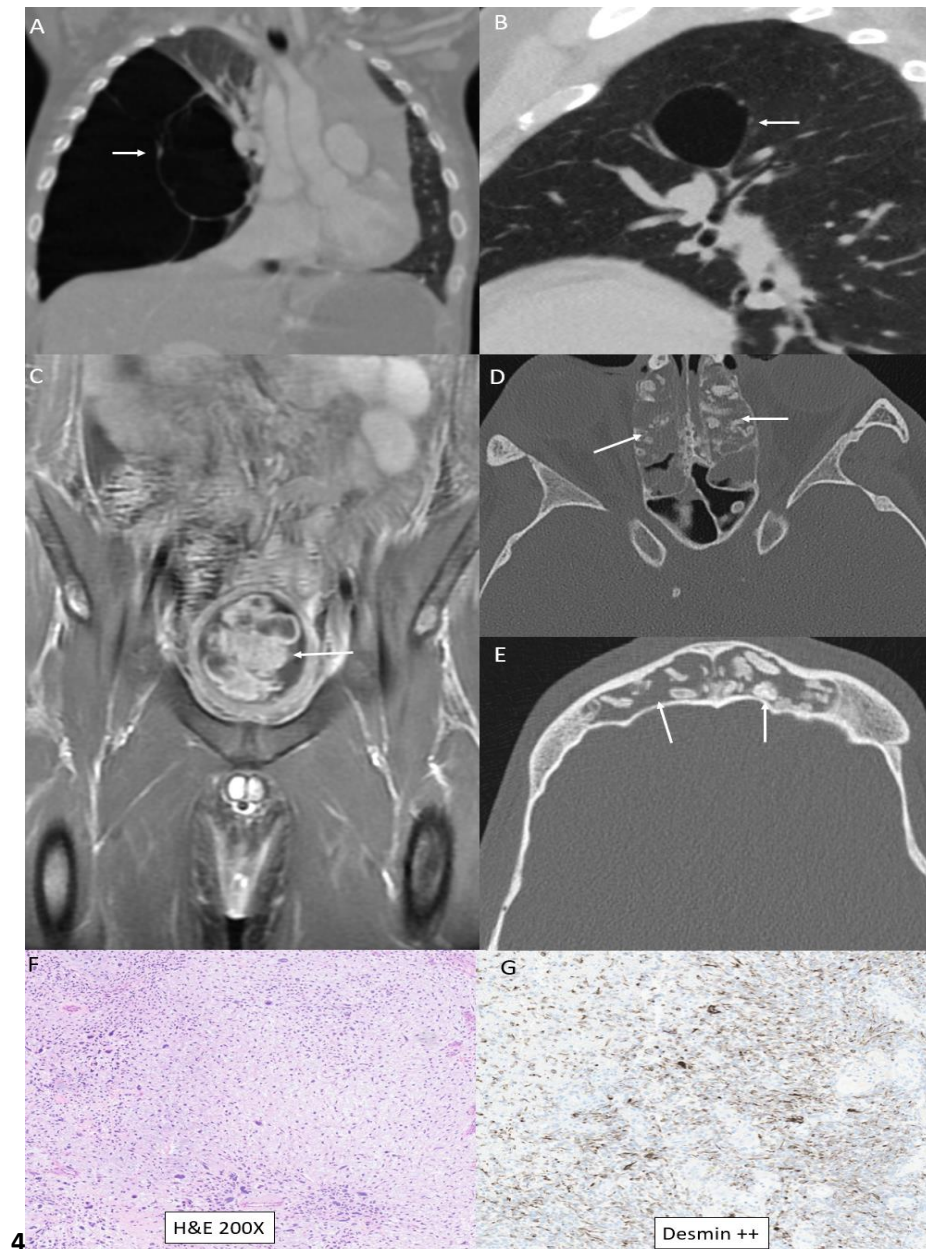
BAP1 tumor predisposition syndrome cancers in different patients. The most common cancers in descending order of frequency are uveal melanoma, malignant mesothelioma, cutaneous melanoma (formerly called atypical Spitz tumors) and renal cell carcinoma. Histopathology on eye enucleation reveals a uveal melanoma (A, *black arrow*) with no involvement of the sclera and distant from the optic nerve. Malignant peritoneal mesothelioma with numerous peritoneal and omental deposits on axial T2-weighted MRI (B, *white arrows*). Cutaneous melanoma (formerly called atypical Spitz tumors) with reddish nodule in the arm (C, *black arrow*). Renal cell carcinoma (clear-cell type) with exophytic right lower renal pole mass on contrast-enhanced coronal CT (D, *white arrow*). These tumors showed loss of BAP1 expression on immunohistochemistry.

Fig 4s



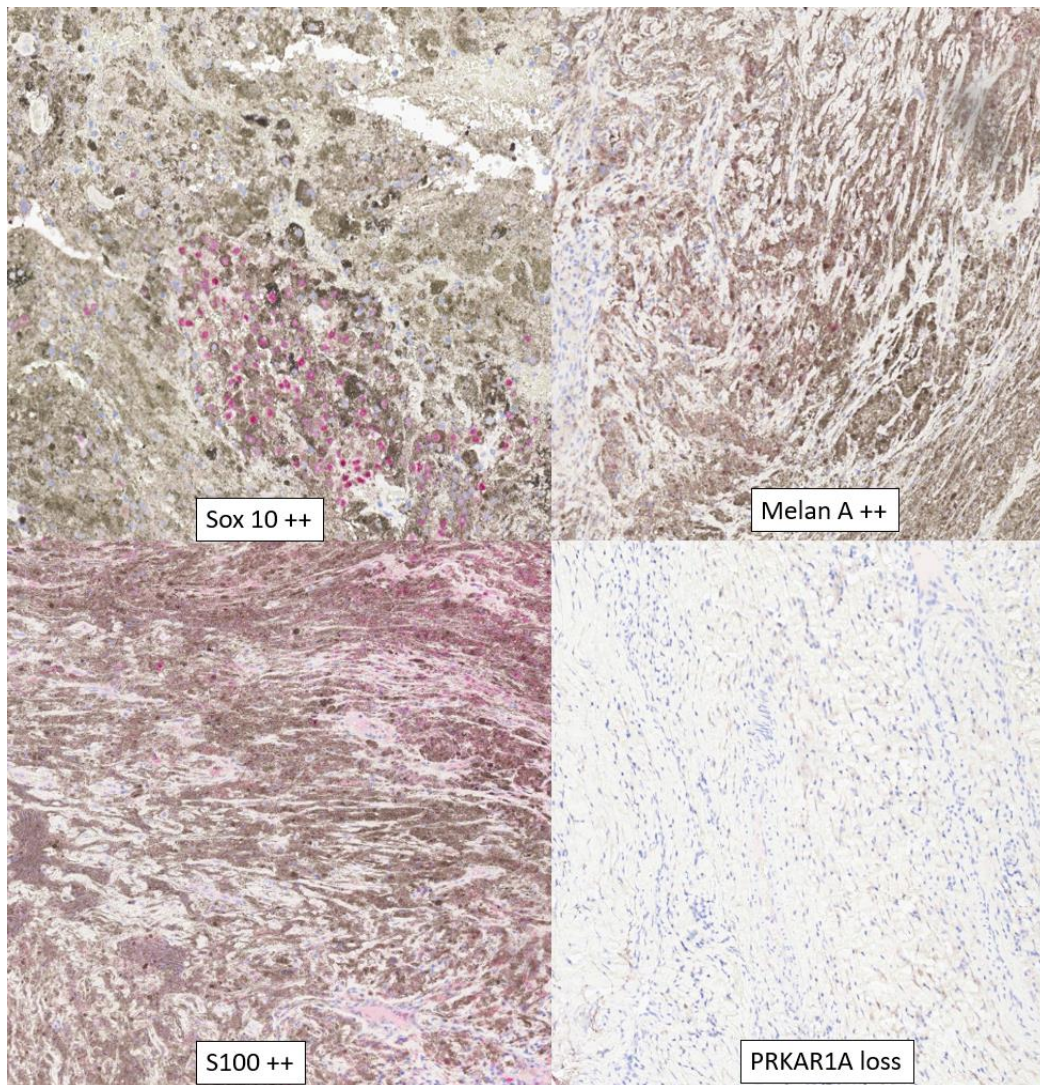
Immunohistochemical studies with loss of BAP1 expression in a patient with lateral cerebellomedullary cistern meningioma (A). Control image with retained expression of BAP1 in a different patient, ruling out BAP1 mutation (B).

Fig 5s



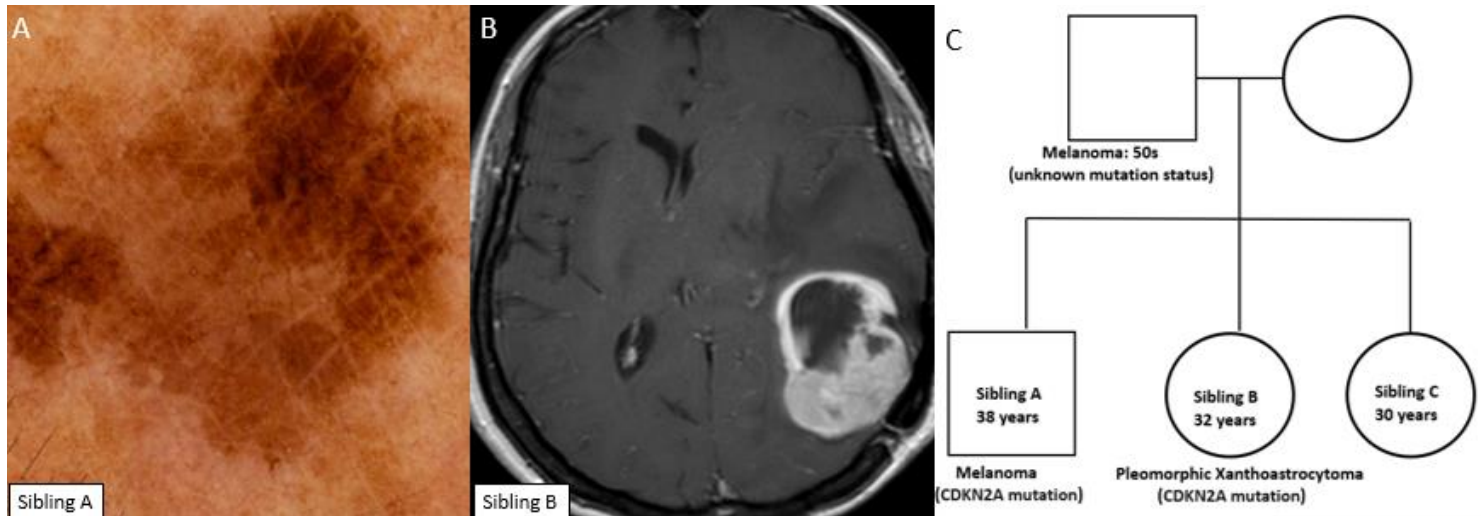
DICER1-mutant tumors: Coronal (A) and sagittal (B) CT images reveal pleuropulmonary blastoma with Type II (solid-cystic morphology with mural nodule, *arrow*) and Type I (regressed) cystic morphology, respectively. Embryonal bladder rhabdomyosarcoma (C, coronal contrast-enhanced MRI, *arrow*) is one of the hallmark tumors associated with DICER mutation. Bladder rhabdomyosarcoma is seen as heterogeneous solid avidly enhancing mass within the bladder lumen. Nasal chondromesenchymal hamartomas in the same patient presenting with extensive soft tissue “masses” in the frontal and ethmoid sinuses on CT (D, E, axial CT bone windows, *arrow*) with calcific/ossific bodies within the matrix. Histopathology of the bladder tumor reveals embryonal rhabdomyosarcoma with diffuse anaplasia and diffusely positive staining for desmin (G) (muscle marker).

Fig 6s



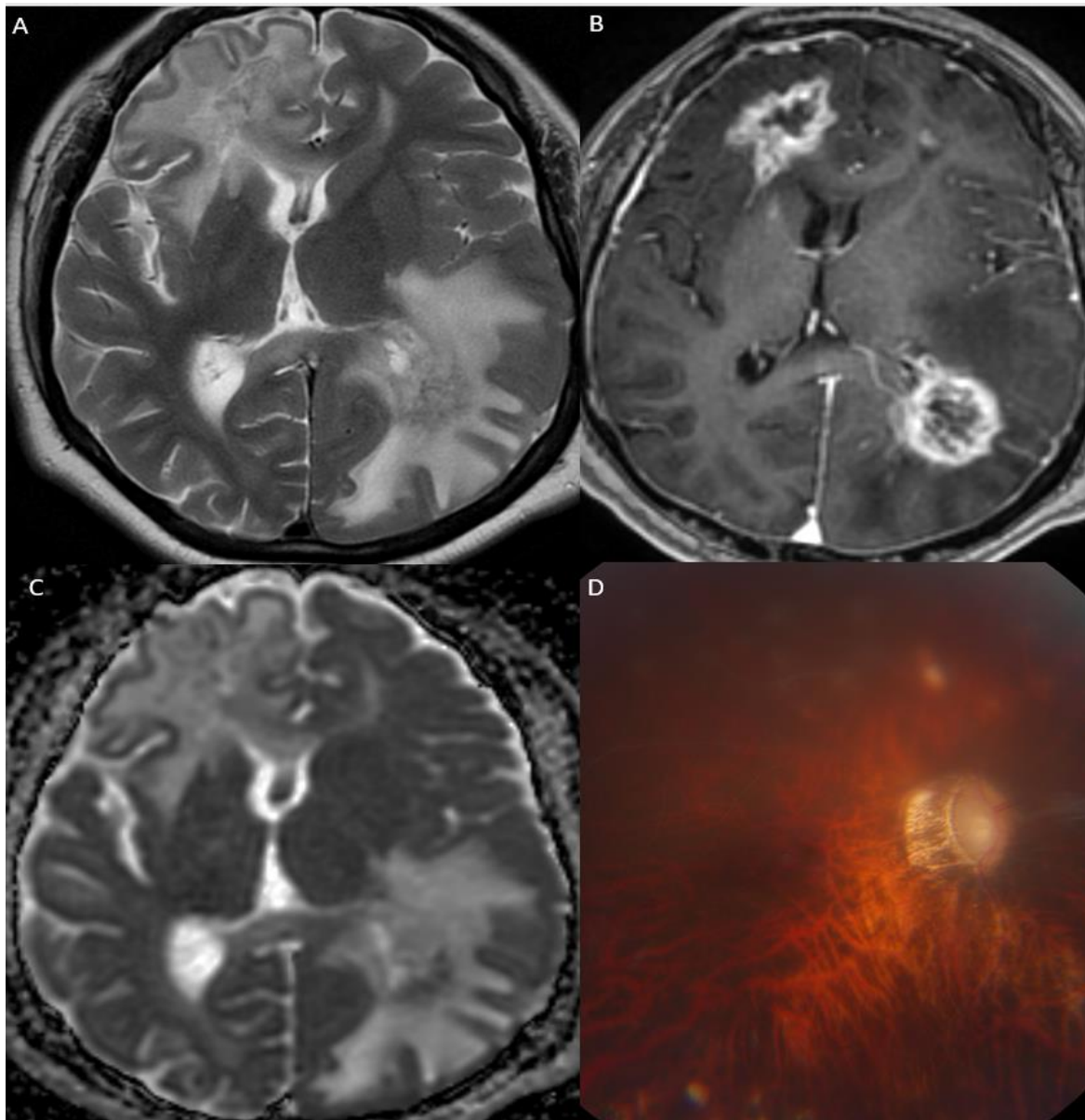
Malignant melanotic nerve sheath tumor (MMNST) in a 26-year-old girl with Carney complex. Immunohistochemistry is positive for SOX10, MelanA, and S100 confirming the diagnosis of MMNST. Neoplastic cells showed complete loss of PRKAR1A, confirming association with Carney complex

Fig 7s



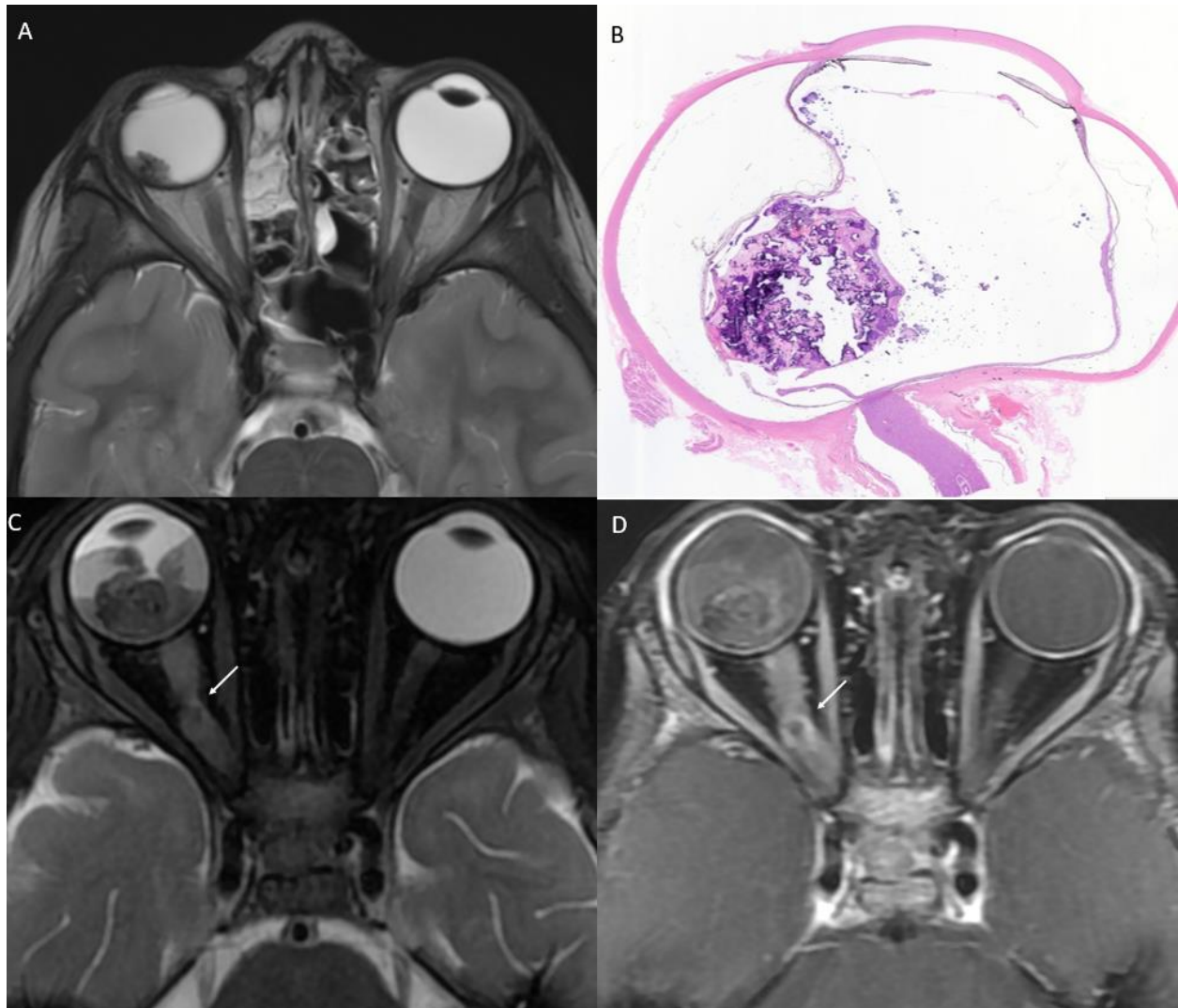
Siblings with CDKN2A mutated melanoma and pleomorphic xanthoastrocytoma, with family history of melanoma. Melanoma along the tibial shin (A) with CDKN2A mutation in sibling A (38-year-old man), with left temporal pleomorphic xanthoastrocytoma in sibling B (32-year-old woman) on axial contrast enhanced MRI. Family pedigree (C) reveals tumors in two generation, although the genetic mutation status in father with melanoma was unknown.

Fig 8s



Cerebroretinal vasculopathy and leukoencephalopathy in a 20-year-old man with Fanconi anemia. Follow-up MRI (A-axial T2-TSE,B axial post-contrast, C-axial ADC map) after six month of immunosuppressive treatment reveals marked reduction in right frontal edema and enhancement with however new areas of edema and enhancement in the left parieto-occipital lobe. Advanced veno-occlusive retinopathy with neovascularization is noted on fundoscopy (D).

Fig 9s



Retinoblastoma in two different children with germline RB1 mutation. Axial T2-weighted MRI (A) in the first patient reveals a right intraocular mass far from the optic nerve and with no extraocular extension, as confirmed on histopathology (B) after enucleation. Different patient with axial T2-weighted (C) and post-contrast (D) images reveals a right intraocular mass with involvement of the optic nerve (C,D, *arrow*) noted as thickening and enhancement of the nerve along with retinal detachment.